DEVELOPMENT OF A LONG LIFE ALUMINIUM BRAZING SHEET ALLOY.

GJ Marshall[1], AJE Flemming[1], A Gray[1] & R Llewellyn[2]
[1] Alcan International Ltd, Banbury Laboratory, Southam Road, Banbury, Oxon OX16 7SP, UK.
[2] Alcan Rolled Products UK, Rogerstone Works, Newport, Gwent, NP1 9YA, UK.

Abstract

The use of aluminium alloys for brazed automotive heat exchangers has increased considerably in the last 15-20 years and new alloys have been developed to meet the demand for improved performance. Higher sheet strength, both during and after brazing, allows sheet downgauging and thus lightweighting of components. This is a key requirement in an industry sensitive to the need for fuel economy and reduced emissions.

Alcan has a developed a new brazing sheet core alloy to meet the industry objectives of higher strength without compromising durability. The metallurgy of this new alloy, through composition and thermomechanical process control, makes use of the diffusion of Si during the brazing cycle to create a sacrificial layer for corrosion protection and the re-solutionizing of an Al-Mn-Cu phase to provide strength during and after brazing. The increased Cu content of the new alloy, contrary to the perceptions of industry, provides additional corrosion protection compared to other long-life alloys.

This paper will consider the metallurgical development of the new alloy, from laboratory experiments to commercial trials. Reference will be made to the control of microstructural features that are important to this new alloy and that create the significantly increased strength without detriment to long-life corrosion performance.

Introduction

Heat exchanger units for automotive engines were, until the 1970's, manufactured from copper and brass. It is only in the last 15-20 years that radiator producers have developed joining techniques suitable for aluminium, ie vacuum and flux brazing (Nocolok™), to utilize the lighter weight of aluminium alloys. The development of aluminium alloys to meet the varied requirements has progressed as the usage of aluminium has increased. This paper deals with the Alcan development of a family of alloys [1, 2, 3] that have enhanced airside corrosion behaviour in combination with high strength to offer long-life to components and hence car manufacturers.

In terms of airside corrosion, ie aggressive salt water environments, conventional aluminium alloys like AA3003 or AA3005 are generally attacked intergranularly and perforation of a tube can occur relatively fast. The intergranular attack is reported [4,5] to be accelerated by the diffusion of silicon, from the cladding, along grain boundaries during the brazing cycle. To prevent this type of attack various approaches have been tried including sheet processing changes [6], in an attempt to modify grain structure and deflect the corrosion path, or the incorporation during hot roll bonding of a sacrificial layer between the cladding and core [7]. The Alcan alloy, X800, is an Al-Mn 3xxx alloy which uses the diffusion of silicon from the cladding to protect the core from

corrosion attack and, as a result, prevent penetration of the tube wall.

The options for strengthening brazing sheet are restricted by the final high temperature joining process which renders ineffective both strain hardening and grain size strengthening. The purpose of this paper is to briefly review the important aspects of X800, Alcan's long life brazing sheet core alloy and detail the development of Alcan's stronger core alloy, X900. Reference will be made to the control of microstructural features that are important to this new alloy and that create the significantly increased strength without detriment to the long-life corrosion behaviour of the parent alloy.

Materials

The present study was performed using material produced in the laboratory at Banbury and commercially by Alcan Rolled Products (UK) at Rogerstone, Gwent. The commercial X800 in this study was single side clad with AA4104 (see Table 1), a clad/core package used in vacuum brazing. However, the microstructural aspects discussed in this report are equally applicable with cladding employed in flux or Nocolok™ brazing (eg. AA 4045, AA 4343 etc.) since X800 can be used in any conventional brazing process.

The typical composition range for X800 and the concentrations for the sheet used in the present investigation are given in Table 1. Each of the main elements is carefully controlled and influences the microstructure of the brazing sheet. The Fe and Si, which are normal impurities in aluminium alloys, are reduced in comparison to standard alloys, AA3003 for example, to restrict the number of coarse constituent particles formed during casting and to aid the corrosion behaviour in a manner described in a subsequent section. Mn is required for solute and dispersion strengthening whilst Cu and Mg are added for solid solution strengthening, though the Cu is also important for corrosion protection (1).

Table I: Typical Alloy Compositions.

Alloy	Si wt%	Fe wt%	Cu wt%	Mn wt%	Mg wt%
X800	0.15max	0.40max	0.60max	0.8-1.5	0.50max
X900	0.15max	0.40max	1.0max	0.8-1.5	0.20max
3003	0.40max	0.70max	0.30max	0.8-1.2	0.05max
X808	0.06	0.19	0.27	1.09	0.21
4104	9-10.5	0.8max	0.25max	0.1max	1.0-2.0

Optical metallography was performed on sheet cold mounted and then polished and etched using standard techniques for aluminium alloys. More detailed studies of precipitate morphology were carried out on thin foils using a JEOL 2000FX transmission electron microscope (TEM). Thin foils were prepared in a twin jet electropolisher using a solution of 5% HNO_3, 1.5% $HClO_4$ in methanol at a current of 100mA and a temperature of less than - 10°C. An electron probe microanalyser (EPMA) was used to characterise the coarse constituent particles in quantitative terms of composition and size.

Two types of corrosion test were performed in the course of this study; Sea Water Acetic Acid Test (SWAAT) (8) is the accepted industry test that simulates the airside service performance of heat exchanger units and can be used to evaluate coupons or full scale units. The second test involves an evaluation of internal or waterside corrosion employing a service simulation rig. A radiator coolant (ASTM D2570-91) is circulated in a chamber containing sheet coupons for 5 days at 88°C followed by 2 days stagnant at 25°C. This cycling continues for a maximum of 7 weeks with coupons removed at intervals for inspection. A measurement of maximum pit depth and pitting frequency is then made for a number of sheet variants.

Results and Discussion

X800 Microstructure

The use of silicon diffusing from the clad layer and the 'receptive' nature of the core microstructure are key elements in the formation of a sacrificial interlayer that gives X800 its long life corrosion performance[2]. Microstructurally it is the distribution of the major alloying elements prior to brazing that is controlled during sheet manufacture by careful thermomechanical processing. Before brazing a clear interface exists between the X800 core and the Si rich cladding alloy that comprises brazing sheet. The Mn in the X800 core is largely distributed between dispersoids and solid solution, although a small amount is contained within the coarse particles formed during casting. The fine dispersoids exhibit an average particle size of 60nm and contain Al, Mn and Si; electron diffraction indicated a cubic crystal structure with a=1.26nm (see reference 2 for details), consistent with the α-Al-Mn-Si phase [9]. There are also occasional coarser particles which contain Al, Fe and Mn and these have a crystal structure compatible with the orthorhombic $(FeMn)Al_6$ phase (again see reference 2 for details). The previous publication[2] also showed that the residual Mn in solid solution was approximately 0.75wt%, measured in the TEM (EDX). This high solute level indicated a relatively low fraction of α-phase compared to, for example, fully homogenised AA3003 sheet[10]. This difference is attributable to the composition and thermomechanical processing of X800; in particular, the low Si content and the ingot heat to roll practice[1].

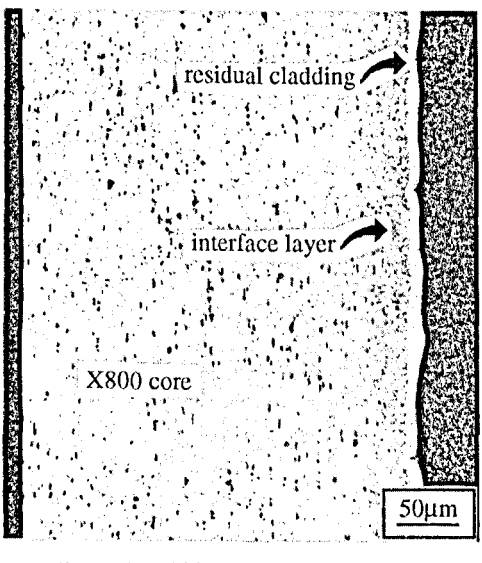

Figure 1: X800 Brazed Microstructure.

After subjecting the sheet to a simulated brazing cycle, distinct changes in microstructure were observed at the interface between the X800 core and the re-solidified cladding. Figure 1 shows the presence of three distinct regions; a residual cladding (etched white) of α-Al and silicon particles, an interface layer (etched dark) and the X800 core (lightly attacked by the etchant). The main feature associated with the formation of the interface layer is the inward diffusion of Si from the Al-Si cladding. The depth of Si diffusion, typically 50-70μm, has been measured by electron microprobe and corresponds well with the width of the interface layer seen by optical metallography. The influx of silicon during the brazing cycle also causes significant microstructural differences between the X800 core and the interface layer which explains the relative etching responses. A previous paper [2] showed that the core of the vacuum brazed sheet had considerably coarser α-AlMnSi precipitates (mean size 122nm) compared to the as-rolled sheet and a significantly reduced number density. The dispersoid density is illustrated in Figure 2(a). In the interface layer, where the Si content is substantially enhanced (EPMA traces suggest up to 1.2wt%), the formation of α-AlMnSi precipitates is encouraged with the result that a dense population of precipitates is formed, Figure 2(b). It is well known that increasing Si concentration reduces the solid solubility of Mn in aluminium [11]. Although the number density was significantly higher, the mean dispersoid size was little different to that in the vacuum brazed core, with a mean of 117nm. The Mn solid solution contents of the matrices in the core and interface region of the X800 were determined by TEM to be 0.93 and 0.45wt% respectively and this reflects the changing Mn solubility with Si content in the two regions of the microstructure.

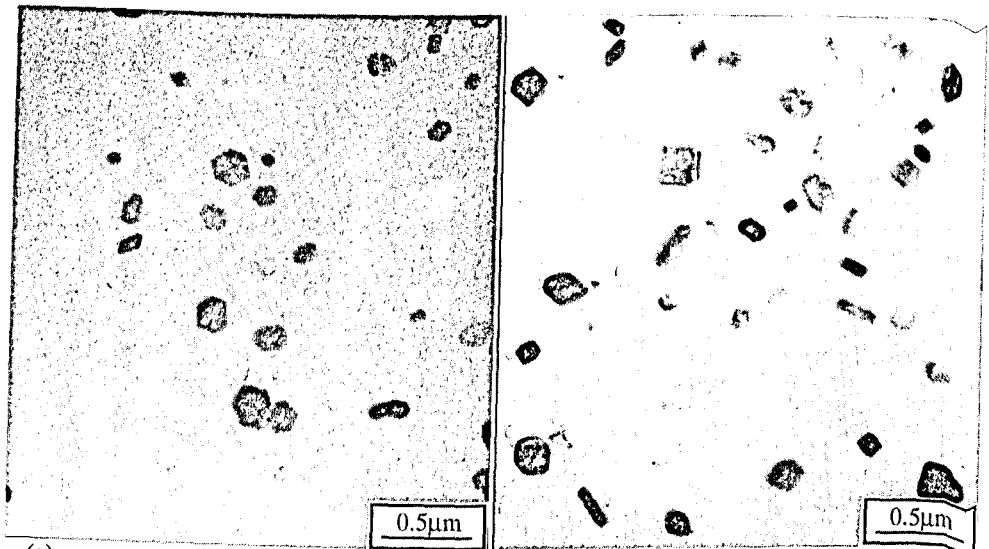

Figure 2: TEM of Brazed X800 showing Dispersoids in the (a) Core and (b) Interface Layer.

The chemistry of the dispersoids and constituent particles was determined in the TEM using a sandwich extraction technique described elsewhere(2). The dissolution process leaves the precipitates sandwiched between two layers of carbon, but the choice of KI avoids chemical attack of the precipitates and thus allows detailed crystallographic and elemental analysis to be performed without matrix contributions. Figure 3(a), which describes the composition of the fine α–AlMnSi dispersoids, reveals an increase in Si content during the brazing cycle both in the core and the interface layer, whereas the Mn content remains relatively stable. The change in silicon content from the as-rolled sheet to the brazed core marks the move towards chemical equilibrium within the dispersoids as a result of the high temperature soak. This takes the Si concentration found in α-phase to within the stoichiometry reported by Mondolfo (11). Figure 3(b) reports similar data for the coarser, constituent particles. These particles, in the as-rolled sheet and the vacuum brazed core, have been identified by Selected Area Diffraction (SAD) in the TEM as the $(FeMn)Al_6$ phase (see reference 2). The Mn and Fe atoms can occupy the same sites in the $(FeMn)Al_6$ structure and therefore the relative amounts of each element in the particles can change. To help clarify the graph, Figure 3(b), an additional column, representing the Mn+Fe content, has been included. It can be seen that the total Fe+Mn content is consistent at about 16 at% as would be expected from $(FeMn)Al_6$. The coarse, constituent particles in the interface layer were found to contain significant levels of Si (average 10.9 at%) and this had the effect of transforming the crystallographic structure from $(FeMn)Al_6$, as in the core, to α-Al(FeMn)Si. The transformation also corresponds to an increase in Fe+Mn content due to higher Mn concentrations as the solid solubility in the matrix decreases. This summary of microstructural differences gives an insight into the metallurgical understanding required to develop the corrosion protection inherent in X800.

The corrosion behaviour of post-brazed X800 was evaluated using the SWAAT environment and corrosion attack was confined to the interface layer between the residual cladding and the core, at times up to 4 weeks exposure. The corrosion first occurred through the grain boundary regions in the residual cladding which are rich in Si and Cu and therefore anodic to the α-aluminium. Once the attack reached the core, the corrosion was confined to the interface layer and hence progressed slowly in a lateral manner thereby protecting the sheet from penetration. In a previous

publication[2], the free corrosion potentials of the two microstructural regions, interface layer and brazed X800 core, were measured. The data showed a small but significant difference in the potentials of the interface layer and core with average values measured as -740 and -720mV respectively. These results confirm that the interface layer is more anodic and hence sacrificial to the core in a salt solution which is representative of the SWAAT environment which, in turn, is believed to simulate service conditions. It is worth noting that the degree of corrosion protection provided by the interface layer is substantial, with large areas of core protected by thin interface layers as attack progresses. The change in corrosion potential by ~20mV is small but demonstrates the potency of such a mechanism.

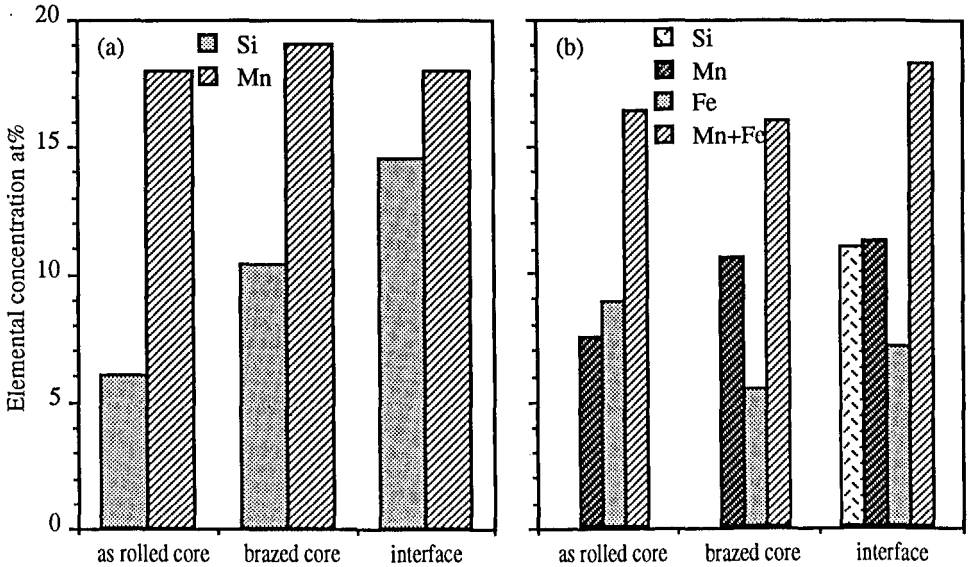

Figure 3: Composition of (a) Dispersoid Particles and (b) Constituent Particles.

X900 Microstructure and Corrosion Behaviour.

The objective of the X900 development was to increase significantly the mechanical performance of a core alloy, including post-brazed strength, without detriment to component manufacture (ie.formability and brazeability) or durability (corrosion). Mechanical stability is required during brazing and strength is needed in service, but the ability to enhance these parameters is not necessarily linked to the same microstructural feature. It is believed that stability at high temperatures during brazing requires the prevention of grain boundary motion, hence the benefit of high aspect ratio grain morphologies. Whilst aluminium alloys can be strengthened by a number of mechanisms, they are not all valid for post-brazed strength since the product is fully recrystallized and generally has a grain size much larger than that required for strengthening. Solid solution strengthening is the most reliable and elements such as Cu, Mg and Mn are often used. Other elements such as Cr, Zr, Ti and V are less frequently used because of their low solid solubility in aluminium; however at low alloying contents their effect on properties is being exploited in other sheet products [12].

Figure 4 demonstrates, from laboratory studies, the effect of solid solution strengthening by Cu and the benefit observed when additional elements were trialled. Magnesium is also an effective strengthener but has to be limited in brazing sheet applications because of problems in flux brazing

furnaces[13]. Commercially, Cu is more acceptable than the use of transition elements in aluminium alloys and, therefore, was chosen as the basis for the stronger X900 core alloy. However two problems were foreseen; firstly Cu in Al alloys is perceived to present a corrosion problem [14] often associated with the formation of $CuAl_2$ particles and solid solution strengthening does not usually aid high temperature stability. The latter point was resolved during initial trials [15] when the sag resistance of X900 was shown to improve when compared to X800. To address the first point and understand the second, a detailed microstructural examination was performed on the new alloy using commercially produced metal from Alcan Rolled Products in Rogerstone.

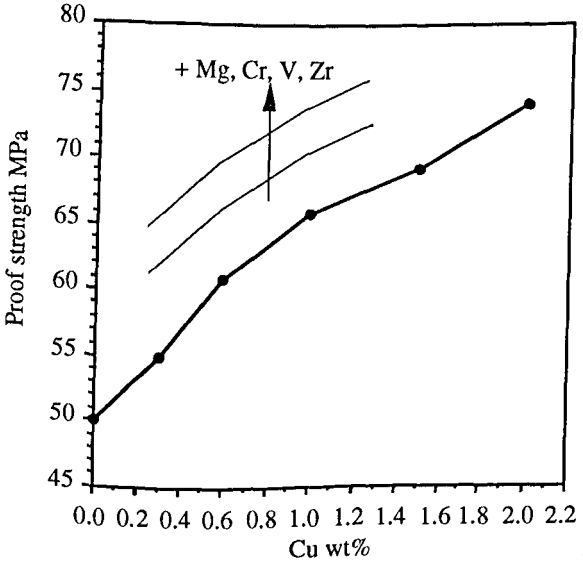

Figure 4: Effect of Alloying on Post-Brazed Strength.

Two questions have been addressed, what does the higher Cu level change in the brazing sheet microstructure and how will this affect properties? Cu in Al alloys segregates strongly during solidification such that pronounced microsegregation (coring) is observed in the cast microstructure, see Figure 5(a). Electronprobe microanalysis (EPMA) of the constituent particles around cell boundaries indicated that whilst Cu was contained in a few, relatively small, intermetallics, the majority remained in solid solution. The feature detection and classification system (FDC) showed that the Cu bearing particles contained little or no Fe and Mn and, thus, it was assumed that the $CuAl_2$ phase had formed. These particles subsequently dissolved during ingot heating to the soak temperature prior to hot rolling and $CuAl_2$ particles were not observed at any further stage in sheet production. A more important feature of the ingot preheating was the formation of dispersoids within the aluminium matrix. Figure 5(b) shows the distribution of the dispersoids and the formation of denuded zones at the cell centres and adjacent to cell boundaries. The presence of the denuded zone in both regions suggests that the microsegregation of elements that form the particles, Cu and Mn (see below), has not been removed prior to precipitation in this low temperature heat treatment.

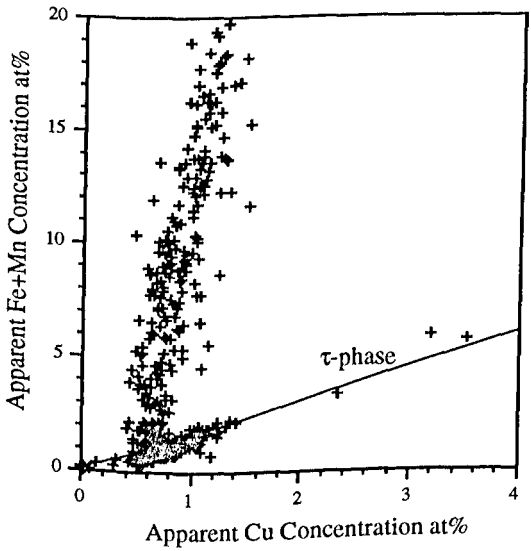

Figure 6: FDC on X900 after Low Temperature Homogenisation. (see text for details)

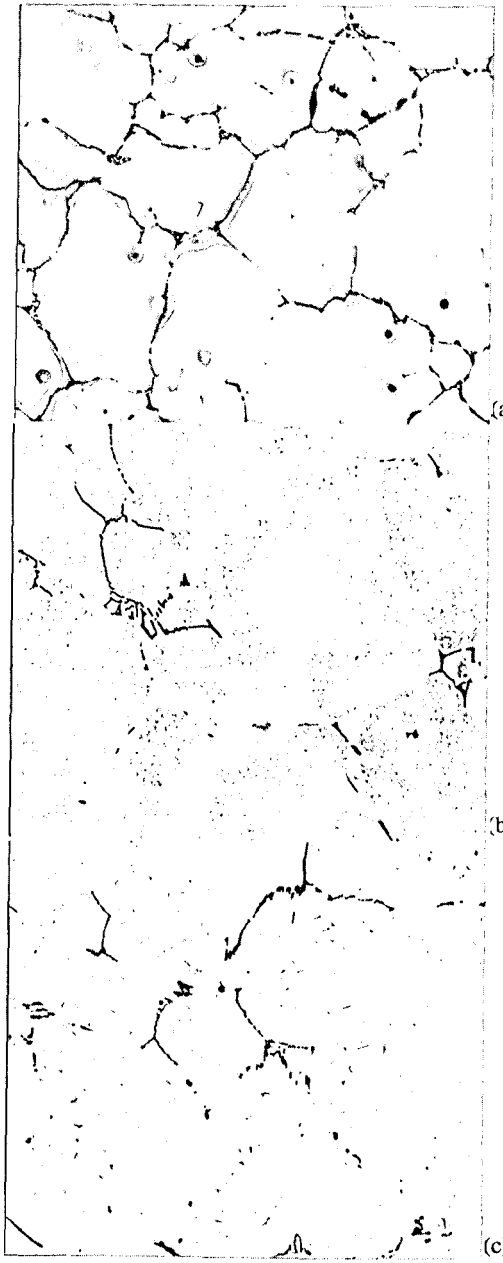

Figure 5: Optical micrographs (etched in 0.5% HF) of X900; (a) As-cast, (b) Low Homogenisation and (c) High Homogenisation Temperature.

FDC analysis on the probe revealed that the majority of fine particles contained Mn and Cu in an apparent ratio of 3:2, see figure 6, whilst the coarse constituents had not altered their composition nor, indeed, their morphology. Electron diffraction in the TEM, figure 7, showed that the fine dispersoids were an $Al_{20}Mn_3Cu_2$ phase with an orthorhombic crystal structure[16], called τ-phase. At high ingot soak temperatures the τ-phase was not found by TEM nor the FDC analysis indicating these particles dissolve at temperatures above 540°C, in agreement with thermodynamic calculations. Figure 5(c) shows that the τ-phase has been replaced by another particulate which has a rod or plate morphology. The dispersoids have grown to large sizes at this temperature but are sparsely populated, as would be expected as solute returns to solid solution. The dispersoids were shown to be $(FeMn)Al_6$ by electron diffraction.

The low temperature ingot heating which is preferred in X800 [1], encourages the retention of τ-phase in X900 during subsequent sheet processing and is present in the alloy prior to brazing of the heat exchanger component. As the τ-phase contains significant amounts of Cu its presence after brazing would be considered detrimental to final strength since it reduces the main solid solution strengthening agent. It is therefore necessary to control the size of the τ-phase during thermomechanical processing to ensure that it has not exceeded the maximum

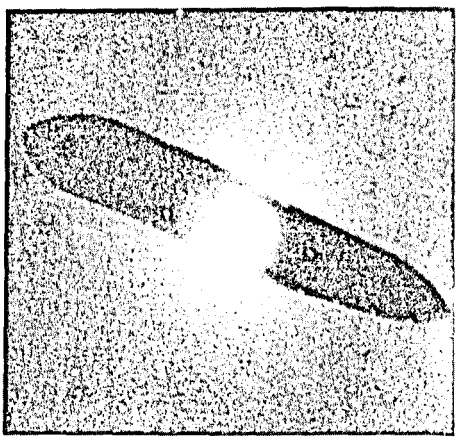

Figure 7: Identification of τ-phase by selected area electron diffraction.

size for dissolution during the short brazing cycle. Furthermore, the presence of significant amounts of fine dispersoids at the onset of brazing could account for the improved sag resistance of X900 when compared with X800. It should be apparent that the important microstructural feature to control in X900 is the dispersoid size. With this control, then a brazing sheet core alloy with a proof strength of 65-70MPa and good high temperature sag resistance can be achieved.

In developing X900, a subsidiary objective was to maintain the excellent corrosion performance developed in X800. The new alloy has been subjected to SWAAT and waterside evaluation. Firstly, it was confirmed by optical metallography and EPMA elemental line scans that the formation of the interface layer during brazing was unaffected by the extra addition of Cu. SWAAT data for X900, X800 and AA3003 tubestock was published by the authors in a recent conference (15) and indicated that the interface layer was providing long-life corrosion protection in X900. Moreover, the higher Cu content of X900 was also shown to enhance the airside corrosion behaviour with slightly better protection than X800. Corrosion potential measurements of the X900 core gave a value of -695mV, more noble than X800 due to additional Cu. The higher Cu will also be present within the interface layer, maintaining the potential difference with the core and, thus, the sacrificial effect of the layer is not compromised. Table II shows the results from waterside testing (ASTM D2570) of the same 3 alloys. It should be clear that AA3003, X800 and X900 have comparable behaviour in this test, therefore confirming that Cu is not detrimental to performance.

Table II: Pitting Depth during Waterside Testing

Alloy	Maximum depth, μm		
	2 weeks	4 weeks	6 weeks
X800	6	8	10
X900	5	10	10
AA3003	10	12	12

Conclusions

- Composition and thermomechanical process control enable X800 to achieve its long-life corrosion protection by the formation of a sacrificial interface layer.
- The addition of Cu to X800 improves the post brazed strength and high temperature sag resistance. The new alloy, X900, requires microstructural control during processing to achieve the correct dispersoid size range for property enhancement as a heat exchanger core alloy.
- In contrast to industry perceptions, the high level of Cu in brazing sheet is not detrimental to corrosion performance and indeed X900 outperforms X800 in the industry standard SWAAT environment.

References

1. Fortin P.E., Marois P.H., Evans D.G.S., US Patent 5,037,707, Aug 1991.
2. Marshall G.J., Bolingbroke R.K., Gray A., Metallurgical Transactions, 24A, 1993, 1935.
3. Gray A., Marshall G.J., European Patent Application 93 302 684.1, April 1993.
4. Schmatz DJ, Welding Research Supplement, (10), 1983, pp 267-271.
5. Wade K.D., Scott D.H.,'Aluminium Technology'86', Ed Sheppard T., I of M, 1986, p 521
6. Finegan W..D, US patent 4,586,964, May 1986.
7. Miller P.R., US patent 2,821,014, Jan 1958.
8. ASTM G85-85, 1992 Annual Book of ASTM Standards, p357.
9. Cooper, M., Robinson, K., Acta Cryst., 20, 1966, p 614.
10. Warlimont H., Aluminium, 53, 1977, p171.
11. Mondolfo L.F., Aluminium Alloys, Structure and Properties., (Butterworths), 1976, p 594.
12. Marshall G.J., Ricks R.A., Limbach P.K.F., Mat. Sci Techn., 7, 1991, p 263.
13. Takigawa J., Okamoto T., Kobelco Tech. Review, 1993, April, 16, p 34.
14. Godard, H.P., The Corrosion of Light Metals, (John Wiley & Sons), New York, 1967.
15. Marshall G.J., Flemming A.J.E., Gray A., Llewellyn R., SAE paper 94-0505, March 1994.
16. Villars P., Calvert L.D., Pearsons Handbook of Crystallographic Data for Intermetallic Phases., 2, 1985, ASM.